

A Comparative Study of Artificial Potential Fields and Safety Filters

Ming Li and Zhiyong Sun

Abstract—In this paper, we have demonstrated that the controllers designed by a classical motion planning tool, namely artificial potential fields (APFs), can be derived from a recently prevalent approach: control barrier function quadratic program (CBF-QP) safety filters. By integrating APF information into the CBF-QP framework, we establish a bridge between these two methodologies. Specifically, this is achieved by employing the attractive potential field as a control Lyapunov function (CLF) to guide the design of the nominal controller, and then the repulsive potential field serves as a reciprocal CBF (RCBF) to define a CBF-QP safety filter. Building on this integration, we extend the design of the CBF-QP safety filter to accommodate a more general class of dynamical models featuring a control-affine structure. This extension yields a special CBF-QP safety filter and a general APF solution suitable for control-affine dynamical models. Through a reach-avoid navigation example, we showcase the efficacy of the developed approaches.

I. INTRODUCTION

Motion planning is a fundamental aspect of robot autonomy, extensively researched over decades and applied across diverse domains such as agriculture [1], warehouse automation [2], and robotic surgery [3]. There are various methodologies for motion planning, broadly categorized into three types according to [4]: sampling-based techniques, optimization-based methods, and reactive motion approaches.

Among these approaches, artificial potential fields (APFs), a form of reactive motion planning, stand as a crucial solution due to their simplicity, versatility, and computational efficiency, especially in real-time obstacle avoidance scenarios [5]. Within this framework, obstacles generate repulsive forces, while goal positions exert attractive forces, guiding the robot along the path of least resistance toward its destination. Over the years, efforts have been directed towards adapting APFs to address increasingly complex scenarios [6]–[8] and refining APFs’ behavior (particularly in addressing undesirable oscillations) [9]. Furthermore, research continues to explore effective methods for motion planning using APFs [10], including their application in UAV motion planning [11].

In recent years, control barrier functions (CBFs), which leverage Lyapunov-like arguments to ensure set forward invariance, have gained significant attention [12], [13]. Due to their efficacy in handling nonlinear systems, suitability for real-time control, and effectiveness in managing high-relative-degree

constraints [14], CBFs have found increasingly popular applications in various safety-critical scenarios, including adaptive cruise control [12], bipedal robot walking [15], and multi-robot coordination [16]. Among existing studies, a prevalent application of CBFs involves formulating quadratic programs (QPs) for controller synthesis [12]. As a result, they are often viewed as optimization-based motion planning techniques.

Regarding these two methodologies, a comparative analysis was first conducted in [17] that attempted to address the question: *How do CBFs compare to APFs for obstacle avoidance tasks?* It has been demonstrated that “APFs represent a particular case of CBFs: given an APF, one can derive a CBF, while the reverse is not necessarily true.” In this paper, we revisit this comparative study and aim to answer the following more fundamental questions:

- *What is the relationship between the CBF-QP safety filter and the APF-designed controller?*
- *How does the CBF-QP safety filter perform as compared to the APF-designed controller for autonomous navigation tasks?*

The major differences between our paper and [17] and the main contributions of this paper lie in the following three aspects:

- 1) Instead of using APFs to derive a zeroing-CBF as in [12], in this paper, we have demonstrated that APFs, including attractive and repulsive potential fields, are valid control Lyapunov functions (CLFs) and reciprocal CBFs (RCBFs).
- 2) In [17], the authors first design a zeroing-CBFs using APFs and then synthesize a controller using a CBF-QP safety filter. The resultant controller is characterized by a similar form to the one designed using APFs. In this paper, we have rigorously proved that APF-designed controllers can be derived from CBF-QP safety filters. This is achieved by integrating the APF information into the CBF-QP framework, wherein the attractive potential field is used as a control Lyapunov function (CLF) to guide the design of the nominal controller, and the repulsive potential field serves as an RCBF.
- 3) Building upon the insights gained from deriving APF-designed controllers from CBF-QP safety filters with a single-integrator dynamical model, we extend the results to a more general class of dynamical models characterized by control-affine structures. This extension leads to a special CBF-QP safety filter and a general APF solution, suitable for a wide range of control-affine dynamical models.

This work was supported in part by a starting grant from Eindhoven Artificial Intelligence Systems Institute (EAIISI), The Netherlands. (*Corresponding author: Ming Li.*)

The authors are with the Department of Electrical Engineering, Eindhoven University of Technology, and also with the Eindhoven Artificial Intelligence Systems Institute, PO Box 513, Eindhoven 5600 MB, The Netherlands. {m.li3, z.sun}@tue.nl

II. PRELIMINARY

In this section, we provide a brief introduction to the APF approach, along with an overview of the concepts of CLFs, CBFs, and CBF-QP safety filters.

A. Artificial Potential Fields

The fundamental idea of the APF is that obstacles within the environment repel the robot, while the goal position exerts an attractive force. Consequently, the robot navigates along the direction of minimum potential energy, influenced by the combined effects of these forces. Although several variations of APF methods exist [6]–[8], our particular focus lies in analyzing the original formulation in [5]. Firstly, consider a control system described by a single-integrator dynamical model:

$$\dot{\mathbf{x}} = \mathbf{u}, \quad (1)$$

where $\mathbf{x} \in \mathbb{R}^n$ is the position, and $\mathbf{u} \in \mathbb{R}^n$ denotes the velocity, serving as the control input for the system. The primary objective is to formulate a desired velocity profile that steers the system towards a specified goal position, while effectively avoiding one or multiple obstacles encountered along the trajectory.

1) *Attractive Potential Field*: Firstly, we denote \mathbf{x}_{goal} as the goal position, which exerts an attractive potential field on the system, represented by:

$$U_{\text{att}}(\mathbf{x}) = \frac{1}{2} K_{\text{att}} \|\mathbf{x} - \mathbf{x}_{\text{goal}}\|^2, \quad (2)$$

where $K_{\text{att}} \in \mathbb{R}_{>0}$ is the attraction constant associated with the attraction potential field. The attraction force is obtained through the gradient of (2), which is given as follows:

$$\mathbf{F}_{\text{att}}(\mathbf{x}) = \nabla U_{\text{att}}(\mathbf{x}) = K_{\text{att}} (\mathbf{x} - \mathbf{x}_{\text{goal}}), \quad (3)$$

where $\nabla U_{\text{att}}(\mathbf{x}) = \frac{\partial U_{\text{att}}}{\partial \mathbf{x}}(\mathbf{x})^\top$.

2) *Repulsive Potential Field*: Any obstacles in the area assert a repulsive potential field, given by

$$U_{\text{rep}}(\mathbf{x}) = \begin{cases} 0, & \rho(\mathbf{x}) \geq \rho_0, \\ \frac{1}{2} K_{\text{rep}} \left(\frac{1}{\rho(\mathbf{x})} - \frac{1}{\rho_0} \right)^2, & \rho(\mathbf{x}) < \rho_0, \end{cases} \quad (4)$$

where $K_{\text{rep}} \in \mathbb{R}_{\geq 0}$ represents the repulsive constant associated with the repulsive potential field, and $\rho_0 \in \mathbb{R}_{>0}$ is a user-defined parameter that determines the size of the region affected by repulsive potential field functions. Additionally, $\rho(\mathbf{x})$ denotes the distance to the obstacle or the distance from a safety area surrounding the obstacle, for instance:

$$\rho(\mathbf{x}) = \|\mathbf{x} - \mathbf{x}_{\text{obs}}\| - r, \quad (5)$$

where \mathbf{x}_{obs} is the position of the obstacle center, and $r \in \mathbb{R}_{>0}$ is the radius of the obstacle. The repulsive force is obtained through the gradient of (4), which is given as follows:

$$\mathbf{F}_{\text{rep}}(\mathbf{x}) = \begin{cases} \mathbf{0}, & \rho(\mathbf{x}) \geq \rho_0, \\ -\frac{K_{\text{rep}}}{\rho(\mathbf{x})^2} \left(\frac{1}{\rho(\mathbf{x})} - \frac{1}{\rho_0} \right) \frac{(\mathbf{x} - \mathbf{x}_{\text{obs}})}{\|\mathbf{x} - \mathbf{x}_{\text{obs}}\|}, & \rho(\mathbf{x}) < \rho_0. \end{cases} \quad (6)$$

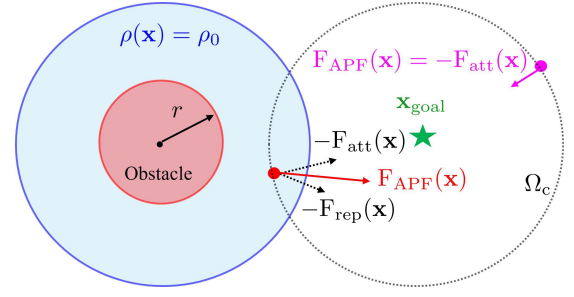


Fig. 1. APF Operational Mechanism: The shaded red area represents an obstacle with radius r , where the solid red circle denotes its boundary. The light blue shaded area illustrates regions where $\rho(\mathbf{x}) < \rho_0$, with the solid blue circle indicating the boundary $\rho(\mathbf{x}) = \rho_0$. The green star denotes the goal position of a navigation task, while Ω_c (black dashed circle) denotes the super level set of the attractive potential field $U_{\text{att}}(\mathbf{x})$. The red solid point signifies the robot, showcasing the force exerted on it when within the region where $\rho(\mathbf{x}) < \rho_0$. Conversely, the magenta solid point depicts the attractive force exerted on the robot when it is situated within the region where $\rho(\mathbf{x}) \geq \rho_0$.

3) *Total Potential Field*: The attractive and repulsive potential fields are combined and the gradient is taken to obtain a feedback controller that pushes the robot to the goal while avoiding obstacles. Specifically, the total force resulting from the APF is the combination of the attractive force (3) and repulsive force (6).

$$\mathbf{F}_{\text{APF}} = -\mathbf{F}_{\text{att}}(\mathbf{x}) - \mathbf{F}_{\text{rep}}(\mathbf{x}). \quad (7)$$

4) *APF Operational Mechanism*: In Fig. 1, we provide a graphical interpretation of APF to explain its operational mechanism. For simplicity, we focus on a scenario featuring only one robot and one obstacle. As shown in Fig. 1, we define the super level set of the attractive potential field to be $\Omega_c = \{\mathbf{x} \in \mathbb{R}^n | U_{\text{att}}(\mathbf{x}) \leq c\}$, where $c \in \mathbb{R}_{>0}$. For the case that the robot (denoted by the red solid point) lies both on Ω_c and in the light blue shaded area, i.e., $\rho(\mathbf{x}) < \rho_0$, the total force on the robot is $\mathbf{F}_{\text{APF}} = -\mathbf{F}_{\text{att}}(\mathbf{x}) - \mathbf{F}_{\text{rep}}(\mathbf{x})$ (red arrow), which is a combination of the force $-\mathbf{F}_{\text{att}}(\mathbf{x})$ and $-\mathbf{F}_{\text{rep}}(\mathbf{x})$ (associated with two dashed arrows in Fig. 1). When $\rho(\mathbf{x}) \geq \rho_0$ (associated with the case that the robot is located on Ω_c while outside the light blue shaded area), the control law is specified as $\mathbf{F}_{\text{APF}} = -\mathbf{F}_{\text{att}}(\mathbf{x})$ (depicted by the magenta arrow), wherein only attractive force is present.

B. CLFs, CBFs, and CBF-QP Safety Filters

Consider a control-affine system [18]

$$\dot{\mathbf{x}} = \mathbf{f}(\mathbf{x}) + \mathbf{g}(\mathbf{x})\mathbf{u}, \quad (8)$$

where $\mathbf{x} \in \mathbb{R}^n$ is the state, $\mathbf{u} \in \mathbb{R}^m$ is the control input, and $\mathbf{f}(\mathbf{x}) : \mathbb{R}^n \rightarrow \mathbb{R}^n$ and $\mathbf{g}(\mathbf{x}) : \mathbb{R}^n \rightarrow \mathbb{R}^{n \times m}$ are continuously differentiable functions, $\mathbf{f}(\mathbf{0}) = \mathbf{0}$. Given a Lipschitz continuous state-feedback controller $\mathbf{k} : \mathbb{R}^n \rightarrow \mathbb{R}^m$, the closed-loop system dynamics are:

$$\dot{\mathbf{x}} = \mathbf{f}_{\text{cl}}(\mathbf{x}) \triangleq \mathbf{f}(\mathbf{x}) + \mathbf{g}(\mathbf{x})\mathbf{k}(\mathbf{x}). \quad (9)$$

Since the functions \mathbf{f} and \mathbf{g} are continuously differentiable, and \mathbf{k} is assumed to be Lipschitz continuous, the function $\mathbf{f}_{\text{cl}}(\mathbf{x})$ is also Lipschitz continuous. Consequently, for any

initial condition $\mathbf{x}_0 = \mathbf{x}(\mathbf{0}) \in \mathbb{R}^n$, there exists a time interval $I(\mathbf{x}_0) = [0, t_{\max})$ such that $\mathbf{x}(t)$ is the unique solution to (9) on $I(\mathbf{x}_0)$.

1) *Control Lyapunov Functions (CLFs)*: CLFs are widely utilized in the design of stabilizing controllers. In this paper, we adopt the standard definition of CLFs as given in [19].

Definition 1. (CLFs [19]) *A continuously differentiable, positive definite, and radially unbounded function $V : \mathbb{R}^n \rightarrow \mathbb{R}_{\geq 0}$ is a CLF for the system (1) if for all $\mathbf{x} \in \mathbb{R}^n \setminus \{\mathbf{0}\}$,*

$$\inf_{\mathbf{u} \in \mathbb{R}^m} [a(\mathbf{x}) + \mathbf{b}(\mathbf{x})\mathbf{u}] < 0, \quad (10)$$

where $a(\mathbf{x}) = L_f V(\mathbf{x})$, $\mathbf{b}(\mathbf{x}) = L_g V(\mathbf{x})$, $L_f V(\mathbf{x}) \triangleq \frac{\partial V(\mathbf{x})}{\partial \mathbf{x}} \mathbf{f}(\mathbf{x})$ and $L_g V(\mathbf{x}) \triangleq \frac{\partial V(\mathbf{x})}{\partial \mathbf{x}} \mathbf{g}(\mathbf{x})$, L_f and L_g denote the Lie derivatives along \mathbf{f} and \mathbf{g} , respectively.

Definition 1 indicates the existence of a state-feedback controller $\mathbf{k}(\mathbf{x})$ that renders the origin of the closed-loop system (8) globally asymptotically stable.

2) *Reciprocal Control Barrier Functions (RCBFs)*: Consider a closed convex set $\mathcal{C} \subset \mathbb{R}^n$ as the 0-superlevel set of a continuously differentiable function $h : \mathbb{R}^n \rightarrow \mathbb{R}$, which is defined as

$$\begin{aligned} \mathcal{C} &\triangleq \{\mathbf{x} \in \mathbb{R}^n : h(\mathbf{x}) \geq 0\}, \\ \partial\mathcal{C} &\triangleq \{\mathbf{x} \in \mathbb{R}^n : h(\mathbf{x}) = 0\}, \\ \text{Int}(\mathcal{C}) &\triangleq \{\mathbf{x} \in \mathbb{R}^n : h(\mathbf{x}) > 0\}, \end{aligned} \quad (11)$$

where we assume that \mathcal{C} is nonempty and has no isolated points, that is, $\text{Int}(\mathcal{C}) \neq \emptyset$ and $\overline{\text{Int}(\mathcal{C})} = \mathcal{C}$.

Definition 2. (Forward Invariance & Safety) *A set $\mathcal{C} \subset \mathbb{R}^n$ is forward invariant if for every $\mathbf{x}_0 \in \mathcal{C}$, the solution to (8) satisfies $\mathbf{x}(t) \in \mathcal{C}$ for all $t \in I(\mathbf{x}_0)$. The system is safe on the set \mathcal{C} if the set \mathcal{C} is forward invariant.*

Definition 3. (RCBFs [20]) *Consider the control system (8) and the set $\mathcal{C} \subset \mathbb{R}^n$ defined by (11) for a continuously differentiable function h . A continuously differentiable function $B : \text{Int}(\mathcal{C}) \rightarrow \mathbb{R}$ is called a RCBF if, for all $\mathbf{x} \in \text{Int}(\mathcal{C})$, there exists class \mathcal{K} functions $\alpha_1, \alpha_2, \alpha$ such that*

$$\frac{1}{\alpha_1(h(\mathbf{x}))} \leq B(\mathbf{x}) \leq \frac{1}{\alpha_2(h(\mathbf{x}))}, \quad (12a)$$

$$\inf_{\mathbf{u} \in \mathbb{R}^m} [c(\mathbf{x}) + \mathbf{d}(\mathbf{x})\mathbf{u}] \leq 0, \quad (12b)$$

where $c(\mathbf{x}) = L_f B(\mathbf{x}) - \alpha(h(\mathbf{x}))$, $\mathbf{d}(\mathbf{x}) = L_g B(\mathbf{x})$.

To illustrate the relationship between the APF-designed controller and the CBF-QP safety filter (which will be discussed in Section III), a sufficient condition of (12b) in the standard RCBF condition (12), which is referred to the condition for defining a tightened CBF in this paper, is introduced as follows:

$$\inf_{\mathbf{u} \in \mathbb{R}^m} [\tilde{c}(\mathbf{x}) + \mathbf{d}(\mathbf{x})\mathbf{u}] \leq 0, \quad (13)$$

where $\tilde{c}(\mathbf{x}) = c(\mathbf{x}) + \Gamma(\mathbf{x})$, $\Gamma(\mathbf{x})$ is a positive semidefinite function. Note that we use the condition (12a) and (13) to define a tightened RCBF.

3) *CBF-QP Safety Filters*: Firstly, we briefly introduce the CBF-QP safety filter, which is defined by the following optimization problem.

$$\mathbf{u}_{\text{CBF}} = \min_{\mathbf{u} \in \mathbb{R}^m} \frac{1}{2} \|\mathbf{u} - \mathbf{u}_{\text{nom}}\|^2 \quad (14a)$$

$$\text{s.t. } \tilde{c}(\mathbf{x}) + \mathbf{d}(\mathbf{x})\mathbf{u} \leq 0, \quad (14b)$$

where \mathbf{u}_{nom} is a nominal controller.

Lemma 1. *The explicit solution to the CBF-QP safety filter, i.e., the optimization problem (14), is:*

$$\mathbf{u}_{\text{CBF}} = \begin{cases} \mathbf{u}_{\text{nom}}, & \mathbf{x} \in \mathcal{S}_{\text{CBF}-1} \cup \tilde{\mathcal{S}}_{\text{CBF}-1}, \\ \mathbf{n}_{\text{CBF}}(\mathbf{x}), & \mathbf{x} \in \mathcal{S}_{\text{CBF}-2}, \end{cases} \quad (15)$$

where

$$\mathbf{n}_{\text{CBF}}(\mathbf{x}) = -\frac{\varphi(\mathbf{x})}{\|\mathbf{d}(\mathbf{x})\|^2} \mathbf{d}(\mathbf{x})^\top, \quad \varphi(\mathbf{x}) = \tilde{c}(\mathbf{x}) + \mathbf{d}(\mathbf{x})\mathbf{u}_{\text{nom}} \quad (16)$$

and

$$\begin{aligned} \mathcal{S}_{\text{CBF}-1} &= \{\mathbf{x} \in \mathbb{R}^n \mid \varphi(\mathbf{x}) < 0\}, \\ \tilde{\mathcal{S}}_{\text{CBF}-1} &= \{\mathbf{x} \in \mathbb{R}^n \mid \varphi(\mathbf{x}) = 0 \text{ and } \mathbf{d}(\mathbf{x}) = \mathbf{0}\}, \\ \mathcal{S}_{\text{CBF}-2} &= \{\mathbf{x} \in \mathbb{R}^n \mid \varphi(\mathbf{x}) \geq 0 \text{ and } \mathbf{d}(\mathbf{x}) \neq \mathbf{0}\}. \end{aligned}$$

Proof. See Appendix A or reference [21]. \square

III. APF VERSUS CBF-QP SAFETY FILTER

In this section, our goal is to obtain a special CBF-QP safety filter by integrating the APF information and bridge the gap between APF and the CBF-QP safety filter, demonstrating that the controller designed using APF is equivalent to the explicit solution of a CBF-QP safety filter.

A. Asymptotic Stability and Safety Guarantees with APFs

Firstly, we demonstrate that the attractive potential field and the repulsive potential field can serve as valid CLF and RCBF correspondingly for a single-integrator model (1). Thereby the attractive force and repulsive force given in (3) and (6) (defined by the gradients of APFs) yield asymptotic stability and safety guarantees, respectively.

Lemma 2. *Consider the single-integrator model (1) and set $V(\mathbf{x}) = U_{\text{att}}(\mathbf{x})$, where $U_{\text{att}}(\mathbf{x})$ is the attractive potential field defined in (2). The control law $\mathbf{u} = -\mathbf{F}_{\text{att}}(\mathbf{x})$, defined by the attractive force given in (3), satisfies the CLF condition (10) and hence ensures the asymptotic stability of the system (1).*

Proof. Firstly, by setting $V(\mathbf{x}) = U_{\text{att}}(\mathbf{x})$ for the dynamical model (1), we obtain $a(\mathbf{x}) = 0$ and $\mathbf{b}(\mathbf{x}) = \mathbf{F}_{\text{att}}(\mathbf{x})^\top$ with Definition 1. Moreover, according to the definition of attractive force in (3), we know that $\|\mathbf{F}_{\text{att}}(\mathbf{x})\|^2 > 0$ for all $\mathbf{x} \in \mathbb{R} \setminus \{\mathbf{x}_{\text{goal}}\}$. Next, we substitute the control law $\mathbf{u} = -\mathbf{F}_{\text{att}}(\mathbf{x})$ into the CLF condition (10), which gives

$$-\mathbf{F}_{\text{att}}(\mathbf{x})^\top \mathbf{F}_{\text{att}}(\mathbf{x}) < 0, \quad \forall \mathbf{x} \in \mathbb{R} \setminus \{\mathbf{x}_{\text{goal}}\}. \quad (17)$$

Then we conclude that the closed-loop system (1) is asymptotically stable. \square

Lemma 3. Consider the single-integrator model (1) and set $B(\mathbf{x}) = \mathbf{U}_{\text{rep}}(\mathbf{x})$ and $h(\mathbf{x}) = \rho(\mathbf{x})$, where the repulsive potential field $\mathbf{U}_{\text{rep}}(\mathbf{x})$ and function $\rho(\mathbf{x})$ are given in (4) and (5), respectively. The control law $\mathbf{u} = -\mathbf{F}_{\text{rep}}(\mathbf{x})$, defined by the repulsive force given in (6), satisfies the RCBF condition and thus ensures the safety of system (1).

Proof. To prove that the repulsive potential field $B(\mathbf{x}) = \mathbf{U}_{\text{rep}}(\mathbf{x})$ with $\mathbf{u} = -\mathbf{F}_{\text{rep}}(\mathbf{x})$ satisfies the RCBF condition, we need to verify that i) $B(\mathbf{x})$ satisfies the condition (12a), and ii) the condition (12b) holds.

Regarding the first aspect, as depicted in Fig. 1, the system remains safe when $\rho(\mathbf{x}) \geq \rho_0$. Then, we examine the situation where $0 \leq \rho(\mathbf{x}) < \rho_0$. In this case, the function $B(\mathbf{x})$ can be formulated as follows:

$$B(\mathbf{x}) = \mathbf{U}_{\text{rep}}(\mathbf{x}) = \frac{1}{\bar{\alpha}(h(\mathbf{x}))}, \quad (18)$$

where

$$\bar{\alpha}(h(\mathbf{x})) = \frac{2}{K_{\text{rep}}} \cdot \left(\frac{\rho_0 h(\mathbf{x})}{\rho_0 - h(\mathbf{x})} \right)^2. \quad (19)$$

Here, it can be verified that $\bar{\alpha}(h(\mathbf{x}))$ is a class \mathcal{K} function when $0 \leq \rho(\mathbf{x}) < \rho_0$ (note that $h(\mathbf{x}) = \rho(\mathbf{x})$), and hence we can always determine class functions $\alpha_1(h(\mathbf{x}))$ and $\alpha_2(h(\mathbf{x}))$ to ensure that the condition (12a) is satisfied.

Furthermore, when $0 \leq \rho(\mathbf{x}) < \rho_0$, according to (6) and (12), we have $c(\mathbf{x}) = -\alpha(h(\mathbf{x}))$ and $\mathbf{d}(\mathbf{x}) = \mathbf{F}_{\text{rep}}(\mathbf{x})^\top$ for the dynamical model (1). By substituting $\mathbf{u} = -\mathbf{F}_{\text{rep}}(\mathbf{x})$ into (12b), it yields

$$-\alpha(h(\mathbf{x})) - \mathbf{F}_{\text{rep}}(\mathbf{x})^\top \mathbf{F}_{\text{rep}}(\mathbf{x}) < 0 \quad (20)$$

since $\|\mathbf{F}_{\text{rep}}(\mathbf{x})\|^2 > 0$ for all $0 \leq \rho(\mathbf{x}) < \rho_0$ (see Equation (6)), which shows that the system (1) is safe. \square

B. Integration of APF in CBF-QP Safety Filter

In this subsection, our objective is to integrate the information from the APF into the CBF-QP safety filter, thereby presenting a special CBF-QP safety filter designed for a safe stabilization task of a single-integrator model. To achieve this, we set the nominal control law to be $\mathbf{u}_{\text{nom}} = -\mathbf{F}_{\text{att}}(\mathbf{x})$ since it ensures asymptotic stability for the system (1) as shown in Lemma 2. Besides, we choose the repulsive potential field to be an RCBF since it ensures the safety guarantees of the system (1) as revealed in Lemma 3.

Proposition 1. Consider the single-integrator model (1). We set $\mathbf{u}_{\text{nom}} = -\mathbf{F}_{\text{att}}(\mathbf{x})$, $B(\mathbf{x}) = \mathbf{U}_{\text{rep}}(\mathbf{x})$, $h(\mathbf{x}) = \rho(\mathbf{x})$, and $\Gamma(\mathbf{x}) = \|\mathbf{F}_{\text{rep}}(\mathbf{x})\|^2 + \alpha(h(\mathbf{x}))$. This yields a special CBF-QP safety filter \mathbf{u}_{ACBF} which follows the definition in (14) with $\mathbf{u}_{\text{nom}} = -\mathbf{F}_{\text{att}}(\mathbf{x})$ and $\tilde{c}(\mathbf{x}) = \|\mathbf{F}_{\text{rep}}(\mathbf{x})\|^2$. Moreover, its explicit solution is given by

$$\mathbf{u}_{\text{ACBF}} = \begin{cases} -\mathbf{F}_{\text{att}}(\mathbf{x}), & \mathbf{x} \in \mathcal{S}_{\text{ACBF-1}} \cup \tilde{\mathcal{S}}_{\text{ACBF-1}}, \\ -\mathbf{F}_{\text{att}}(\mathbf{x}) - \mathbf{F}_{\text{rep}}(\mathbf{x}), & \mathbf{x} \in \mathcal{S}_{\text{ACBF-2}}, \end{cases} \quad (21)$$

where

$$\begin{aligned} \mathcal{S}_{\text{ACBF-1}} &= \{\mathbf{x} \in \mathbb{R}^n \mid \|\mathbf{F}_{\text{rep}}(\mathbf{x})\|^2 - \mathbf{F}_{\text{rep}}(\mathbf{x})^\top \mathbf{F}_{\text{att}}(\mathbf{x}) < 0\}, \\ \tilde{\mathcal{S}}_{\text{ACBF-1}} &= \{\mathbf{x} \in \mathbb{R}^n \mid \mathbf{F}_{\text{rep}}(\mathbf{x}) = \mathbf{0}\}, \\ \mathcal{S}_{\text{ACBF-2}} &= \{\mathbf{x} \in \mathbb{R}^n \mid \|\mathbf{F}_{\text{rep}}(\mathbf{x})\|^2 - \mathbf{F}_{\text{rep}}(\mathbf{x})^\top \mathbf{F}_{\text{att}}(\mathbf{x}) \geq 0 \\ &\quad \text{and } \mathbf{F}_{\text{rep}}(\mathbf{x}) \neq \mathbf{0}\}. \end{aligned}$$

Proof. By setting $B(\mathbf{x}) = \mathbf{U}_{\text{rep}}(\mathbf{x})$ and $h(\mathbf{x}) = \rho(\mathbf{x})$, we derive $c(\mathbf{x}) = -\alpha(h(\mathbf{x}))$ and $\mathbf{d}(\mathbf{x}) = \mathbf{F}_{\text{rep}}(\mathbf{x})$ for the dynamical model (1), following Definition 3. Subsequently, employing the definition of the tightened RCBF in (13), we further determine $\tilde{c}(\mathbf{x}) = \|\mathbf{F}_{\text{rep}}(\mathbf{x})\|^2$ with $\Gamma(\mathbf{x}) = \|\mathbf{F}_{\text{rep}}(\mathbf{x})\|^2 + \alpha(h(\mathbf{x}))$. Then, since $\mathbf{u}_{\text{nom}} = -\mathbf{F}_{\text{att}}(\mathbf{x})$ and $\tilde{c}(\mathbf{x}) = \|\mathbf{F}_{\text{rep}}(\mathbf{x})\|^2$, a special CBF-QP safety filter can be defined according to (14). Following this, as per Lemma 1, the solution to the special CBF-QP safety filter (15) gives a control law as in (21). \square

C. APF-Designed Controller: A Special CBF-QP Safety Filter

In this subsection, we aim to show the relationships between the APF-designed controller and the CBF-QP safety filter. By introducing Assumption 1 (which will be introduced later), we show that the controller designed with APF is equivalent to the controller defined by the special CBF-QP safety filter as presented in Proposition 1.

Assumption 1. Define $\mathcal{G} \triangleq \{\mathbf{x} \in \mathbb{R}^n \mid \rho(\mathbf{x}) < \rho_0\}$. We assume that, for each $\mathbf{x} \in \mathcal{G}$, it holds $\mathcal{S}_{\text{ACBF-1}} = \emptyset$, where $\mathcal{S}_{\text{ACBF-1}}$ is defined in Equation (21).

Proposition 2. Consider the single-integrator model (1). We set $\mathbf{u}_{\text{nom}} = -\mathbf{F}_{\text{att}}(\mathbf{x})$, $B(\mathbf{x}) = \mathbf{U}_{\text{rep}}(\mathbf{x})$, $h(\mathbf{x}) = \rho(\mathbf{x})$, and $\Gamma(\mathbf{x}) = \|\mathbf{d}(\mathbf{x})\|^2 + \alpha(h(\mathbf{x}))$. Moreover, we assume that Assumption 1 holds. Then the controller designed with APF, i.e., (7), is equivalent to the controller defined by the special CBF-QP safety filter given in Equation (21).

Proof. According to Proposition 1, we obtain a special CBF-QP safety filter \mathbf{u}_{ACBF} defined by (21). For the domain $\tilde{\mathcal{S}}_{\text{ACBF-1}}$, it was shown in (6) that $\mathbf{F}_{\text{rep}}(\mathbf{x}) = \mathbf{0}$ holds if and only if $\rho(\mathbf{x}) \geq \rho_0$. Therefore, the set $\tilde{\mathcal{S}}_{\text{ACBF-1}}$ can equivalently be defined by $\tilde{\mathcal{S}}_{\text{ACBF-1}} = \{\mathbf{x} \in \mathbb{R}^n \mid \rho(\mathbf{x}) \geq \rho_0\}$. With regard to the case that $\rho(\mathbf{x}) < \rho_0$, as shown in (21), there are two cases that need to be considered, i.e., $\mathbf{x} \in \mathcal{S}_{\text{ACBF-1}}$ and $\mathbf{x} \in \mathcal{S}_{\text{ACBF-2}}$. While with Assumption 1, $\mathcal{S}_{\text{ACBF-1}} = \emptyset$, thus the controller \mathbf{u}_{ACBF} defined in (21) is specialized to the controller designed by APF in (7), i.e., $\mathbf{u} = \mathbf{F}_{\text{APF}} = -\mathbf{F}_{\text{att}}(\mathbf{x}) - \mathbf{F}_{\text{rep}}(\mathbf{x})$. \square

Remark 1. With the special CBF-QP safety filter \mathbf{u}_{ACBF} as defined in (21), Assumption 1 can be satisfied by appropriately setting ρ_0 . However, there are certain scenarios where Assumption 1 may not hold. It is crucial to emphasize that the introduction of Assumption 1 in this paper aims to establish an equivalence between the APF-designed controller and the CBF-QP safety filter under a certain condition, which does not need to hold at all times. If this assumption does not hold, the main distinctions between the APF-designed controller and CBF-QP safety filter arise when $\rho(\mathbf{x}) < \rho_0$. For the APF approach, the control input is defined by

$F_{\text{APF}} = -F_{\text{rep}}(\mathbf{x}) - F_{\text{rep}}(\mathbf{x})$, while for the CBF-QP safety filter (cf. (21)), the control law is characterized by $-F_{\text{att}}(\mathbf{x})$ and $F_{\text{rep}}(\mathbf{x}) - F_{\text{rep}}(\mathbf{x})$, respectively, when $\mathbf{x} \in \mathcal{S}_{\text{ACBF}-1}$ and $\mathbf{x} \in \mathcal{S}_{\text{ACBF}-2}$.

Remark 2. From another perspective, when Assumption 1 is violated, i.e., $\mathcal{S}_{\text{ACBF}-1} \neq \emptyset$, the APF-designed controller can be interpreted as a special result of the CBF-QP safety filter \mathbf{u}_{ACBF} as given in (21). Specifically, when $\rho(\mathbf{x}) < \rho_0$, one can obtain the APF-designed controller by enforcing $\mathbf{u}_{\text{ACBF}} = -F_{\text{att}}(\mathbf{x}) - F_{\text{rep}}(\mathbf{x})$ when $\mathcal{S}_{\text{ACBF}-1} \neq \emptyset$ in (21). Importantly, introducing this operation to the CBF-QP safety filter gives the APF-designed controller but does not compromise its safety guarantees. We can prove that the APF-designed controllers have strict safety guarantees. In particular, when $h(\mathbf{x}) = 0$ (indicating the robot arrives at the boundary of the obstacle), we have $\|F_{\text{rep}}(\mathbf{x})\| = \infty$, as shown in (6). Consequently, the CBF condition (12) remains satisfied at all times. To be more precise, we substitute $F_{\text{APF}}(\mathbf{x}) = -F_{\text{att}}(\mathbf{x}) - F_{\text{rep}}(\mathbf{x})$ into (12), it gives

$$\begin{aligned} & -\alpha(h(\mathbf{x})) - F_{\text{rep}}(\mathbf{x})^\top (F_{\text{att}}(\mathbf{x}) + F_{\text{rep}}(\mathbf{x})) \\ &= -F_{\text{rep}}(\mathbf{x})^\top (F_{\text{att}}(\mathbf{x}) + F_{\text{rep}}(\mathbf{x})) \\ &= -F_{\text{rep}}(\mathbf{x})^\top (F_{\text{rep}}(\mathbf{x})) = -\infty < 0 \end{aligned} \quad (22)$$

when $h(\mathbf{x}) = 0$.

IV. EXTENSIONS TO CONTROL-AFFINE DYNAMICAL MODELS

As demonstrated in Proposition 1, integrating APF information allows for the design of a special CBF-QP safety filter and building strong connections between the two approaches. This idea can be straightforwardly extended to deal with dynamical models with a control-affine structure. Moreover, as per Proposition 2, a general APF solution for control-affine dynamic models can also be obtained under an assumption similar to Assumption 1.

A. Nominal Control Law for Stabilizing Control

For the dynamical model (8), our first step is to design a nominal control law \mathbf{u}_{nom} for (8) using the attractive potential field as a CLF. To achieve this, we introduce a sufficient condition for the standard CLF condition (10), named as tightened CLF condition, which is expressed as:

$$\inf_{\mathbf{u} \in \mathbb{R}^m} [\tilde{a}(\mathbf{x}) + \mathbf{b}(\mathbf{x})\mathbf{u}] \leq 0, \quad (23)$$

where $\tilde{a}(\mathbf{x}) = a(\mathbf{x}) + \sigma(\mathbf{x})$, $a(\mathbf{x})$ is defined in (10), and $\sigma(\mathbf{x})$ is a positive definite function.

Lemma 4. Consider the dynamic model (1) and set $V(\mathbf{x}) = U_{\text{att}}(\mathbf{x})$, where $U_{\text{att}}(\mathbf{x})$ is the attractive potential field defined in (2). The control law defined by the following optimization problem satisfies the CLF condition (10) and ensures the asymptotic stability of the system (8).

$$\mathbf{u}_{\text{CLF}} = \min_{\mathbf{u} \in \mathbb{R}^m} \frac{1}{2} \|\mathbf{u}\|^2 \quad (24a)$$

$$\text{s.t. } \tilde{a}(\mathbf{x}) + \mathbf{b}(\mathbf{x})\mathbf{u} \leq 0, \quad (24b)$$

where $\tilde{a}(\mathbf{x}) = a(\mathbf{x}) + \sigma(\mathbf{x})$, $a(\mathbf{x}) = L_f V(\mathbf{x})$, $\sigma(\mathbf{x}) = \|\mathbf{b}(\mathbf{x})\|^2$, $\mathbf{b}(\mathbf{x}) = F_{\text{att}}(\mathbf{x})^\top$, and the explicit solution to (24) is:

$$\mathbf{u}_{\text{CLF}} = \begin{cases} \mathbf{0}, & \mathbf{x} \in \mathcal{S}_{\text{CLF}-1} \cup \tilde{\mathcal{S}}_{\text{CLF}-1}, \\ \mathbf{m}(\mathbf{x}), & \mathbf{x} \in \mathcal{S}_{\text{CLF}-2}, \end{cases} \quad (25)$$

where

$$\mathbf{m}(\mathbf{x}) = -\frac{\tilde{a}(\mathbf{x})}{\|\mathbf{b}(\mathbf{x})\|^2} \mathbf{b}(\mathbf{x})^\top, \quad (26)$$

and

$$\begin{aligned} \mathcal{S}_{\text{CLF}-1} &= \{\mathbf{x} \in \mathbb{R}^n | \tilde{a}(\mathbf{x}) < 0\}, \\ \tilde{\mathcal{S}}_{\text{CLF}-1} &= \{\mathbf{x} \in \mathbb{R}^n | \tilde{a}(\mathbf{x}) = 0 \text{ and } \mathbf{b}(\mathbf{x}) = \mathbf{0}\}, \\ \mathcal{S}_{\text{CLF}-2} &= \{\mathbf{x} \in \mathbb{R}^n | \tilde{a}(\mathbf{x}) \geq 0 \text{ and } \mathbf{b}(\mathbf{x}) \neq \mathbf{0}\}. \end{aligned} \quad (27)$$

Proof. As noticed, the constraint (24b) serves as a sufficient condition for the standard CLF condition (10). Consequently, the solution to (24) guarantees the satisfaction of the CLF condition, thereby ensuring the asymptotic stability of the closed-loop system (8). Moreover, the solution to the optimization problem (24) can be obtained by setting $\mathbf{u}_{\text{nom}} = \mathbf{0}$ in (14) and replacing $\tilde{a}(\mathbf{x})$ and $\mathbf{b}(\mathbf{x})$ with $\tilde{c}(\mathbf{x})$ and $\mathbf{d}(\mathbf{x})$, respectively. \square

Remark 3. Note that, in (24), any positive definite function $\sigma(\mathbf{x})$ enables the derivation of a nominal controller satisfying the CLF condition (10) and ensuring the asymptotic stability of system (8). We specifically choose $\sigma(\mathbf{x}) = \|\mathbf{b}(\mathbf{x})\|^2$ in Lemma 4. This choice is by realizing that setting $\sigma(\mathbf{x}) = \|\mathbf{b}(\mathbf{x})\|^2$ in (24) yields a nominal control law $\mathbf{u}_{\text{CLF}} = -F_{\text{att}}(\mathbf{x})$ for a single-integrator model, which aligns with the selection made in Proposition 1.

B. CBF-QP Safety Filter with APF

By following the formulation in Proposition 1, we propose to derive a CBF-QP safety filter with APF for a more general dynamical model, i.e., the dynamical model with control-affine structure as given in (8). As a result, the following proposition is provided.

Proposition 3. Consider the dynamical model (8). We set $\mathbf{u}_{\text{nom}} = \mathbf{u}_{\text{CLF}}$ (given by (24)), $B(\mathbf{x}) = \mathbf{U}_{\text{rep}}(\mathbf{x})$, $h(\mathbf{x}) = \rho(\mathbf{x})$, and $\Gamma(\mathbf{x}) = \|F_{\text{rep}}(\mathbf{x})\|^2 + \alpha(h(\mathbf{x}))$ for the CBF-QP safety filter as given in (14). This yields a special CBF-QP safety filter \mathbf{u}_{AC} that follows the definition in (14), where its explicit solution is expressed as:

$$\mathbf{u}_{\text{AC}} = \begin{cases} \mathbf{u}_{\text{CLF}}, & \mathbf{x} \in \mathcal{S}_{\text{AC}-1} \cup \tilde{\mathcal{S}}_{\text{AC}-1}, \\ \mathbf{n}_{\text{AC}}(\mathbf{x}), & \mathbf{x} \in \mathcal{S}_{\text{AC}-2}, \end{cases} \quad (28)$$

where

$$\mathbf{n}_{\text{AC}}(\mathbf{x}) = -\frac{\varphi(\mathbf{x})}{\|\mathbf{d}(\mathbf{x})\|^2} \mathbf{d}(\mathbf{x})^\top, \varphi(\mathbf{x}) = \tilde{c}(\mathbf{x}) + \mathbf{d}(\mathbf{x})\mathbf{u}_{\text{CLF}},$$

$\tilde{c}(\mathbf{x}) = c(\mathbf{x}) + \Gamma(\mathbf{x})$ ($c(\mathbf{x})$ is defined in (12)), $\mathbf{d}(\mathbf{x}) = F_{\text{rep}}(\mathbf{x})^\top$, and

$$\mathcal{S}_{\text{AC}-1} = \{\mathbf{x} \in \mathbb{R}^n | \varphi(\mathbf{x}) < 0\},$$

$$\tilde{\mathcal{S}}_{\text{AC}-1} = \{\mathbf{x} \in \mathbb{R}^n | \varphi(\mathbf{x}) = 0 \text{ and } \mathbf{d}(\mathbf{x}) = \mathbf{0}\},$$

$$\mathcal{S}_{\text{AC}-2} = \{\mathbf{x} \in \mathbb{R}^n | \varphi(\mathbf{x}) \geq 0 \text{ and } \mathbf{d}(\mathbf{x}) \neq \mathbf{0}\}.$$

Proof. With the above settings, we can easily obtain $\tilde{c}(\mathbf{x}) = c(\mathbf{x}) + \Gamma(\mathbf{x})$ and $\mathbf{d}(\mathbf{x}) = \mathbf{F}_{\text{rep}}(\mathbf{x})^\top$ based on (12) and (13). Afterward, with $\mathbf{u}_{\text{nom}} = \mathbf{u}_{\text{CLF}}$, a special CBF-QP safety filter for a dynamical model with control-affine structure, i.e., \mathbf{u}_{AC} , is defined by following the formulation in (14). Next, with Lemma 1, the explicit solution to the special CBF-QP safety filter, i.e., (28), is obtained. \square

C. Extend APF to a Control-Affine Dynamical Model

Following Assumption 1, we introduce the following assumption to obtain a more generic APF for a control-affine dynamic model.

Assumption 2. Define $\mathcal{G} \triangleq \{\mathbf{x} \in \mathbb{R}^n | \rho(\mathbf{x}) < \rho_0\}$. We assume that, for each $\mathbf{x} \in \mathcal{G}$, there always exists $\mathcal{S}_{\text{AC}-1} = \emptyset$, where $\mathcal{S}_{\text{AC}-1}$ is defined in (28).

Proposition 4. Suppose that Assumption 2 holds for the CBF-QP safety filter \mathbf{u}_{AC} given in (28). A generalized APF applicable to a control-affine dynamic model is derived as follows.

$$\mathbf{u}_{\text{APF-AC}} = \begin{cases} \mathbf{u}_{\text{CLF}}, & \rho(\mathbf{x}) > \rho_0, \\ \mathbf{n}_{\text{AC}}(\mathbf{x}), & \rho(\mathbf{x}) \leq \rho_0, \end{cases} \quad (29)$$

Proof. Referring to (12), we deduce that $c(\mathbf{x}) = L_{\mathbf{f}}B(\mathbf{x}) - \alpha(h(\mathbf{x}))$. By using $\tilde{c}(\mathbf{x}) = c(\mathbf{x}) + \Gamma(\mathbf{x})$ with $\Gamma(\mathbf{x}) = \|\mathbf{F}_{\text{rep}}(\mathbf{x})\|^2 + \alpha(h(\mathbf{x}))$ as per Proposition 3, we obtain $\tilde{c}(\mathbf{x}) = L_{\mathbf{f}}B(\mathbf{x}) + \|\mathbf{F}_{\text{rep}}(\mathbf{x})\|^2$ and $\mathbf{d}(\mathbf{x}) = \mathbf{F}_{\text{rep}}(\mathbf{x})^\top$. With these, it gives the CBF-QP safety filter \mathbf{u}_{AC} given in (28).

Firstly, we consider the case that $\mathbf{x} \in \mathcal{S}_{\text{AC}-1}$. Since $\mathbf{d}(\mathbf{x}) = \mathbf{F}_{\text{rep}}(\mathbf{x})^\top = \mathbf{0}$ if and only if $\rho(\mathbf{x}) \geq \rho_0$, it follows that $\mathbf{U}_{\text{rep}}(\mathbf{x}) = B(\mathbf{x}) = 0$ based on (4). Consequently, we have $\tilde{c}(\mathbf{x}) = 0$ and $\mathbf{d}(\mathbf{x}) = \mathbf{0}$, resulting in $\varphi(\mathbf{x}) = 0$. Thus, the set $\mathcal{S}_{\text{AC}-1}$ can be equivalently defined as $\mathcal{S}_{\text{AC}-1} = \{\mathbf{x} \in \mathbb{R}^n | \rho(\mathbf{x}) \geq \rho_0\}$. When $\rho(\mathbf{x}) < \rho_0$, as specified in (28), we need to consider two cases: $\mathbf{x} \in \mathcal{S}_{\text{AC}-1}$ and $\mathbf{x} \in \mathcal{S}_{\text{AC}-2}$. With Assumption 2, it follows that $\mathcal{S}_{\text{AC}-1} = \emptyset$, leading to the specialization of the controller \mathbf{u}_{AC} defined in (28) to the controller designed by APF in (29), denoted as $\mathbf{u}_{\text{APF-AC}}$. \square

Remark 4. The control law $\mathbf{u}_{\text{APF-AC}}$ defined in (29) can be specialized to $\mathbf{F}_{\text{APF}} = -\mathbf{F}_{\text{att}}(\mathbf{x}) - \mathbf{F}_{\text{rep}}(\mathbf{x})$ when considering a single-integrator model. Firstly, as noted in Remark 3, the nominal control law is $\mathbf{u}_{\text{CLF}} = -\mathbf{F}_{\text{att}}(\mathbf{x})$ for a single-integrator model. Subsequently, we know that, for a single-integrator model, $\tilde{c}(\mathbf{x}) = \|\mathbf{d}(\mathbf{x})\|^2 = \|\mathbf{F}_{\text{rep}}(\mathbf{x})\|^2$ and $\mathbf{d}(\mathbf{x}) = \mathbf{F}_{\text{rep}}(\mathbf{x})^\top$ as demonstrated in Proposition 1, and hence we derive $\mathbf{n}_{\text{AC}}(\mathbf{x}) = -\mathbf{F}_{\text{att}}(\mathbf{x}) - \mathbf{F}_{\text{rep}}(\mathbf{x})$. Based on the above analysis and with (29), it follows that $\mathbf{u}_{\text{APF-AC}} = -\mathbf{F}_{\text{att}}(\mathbf{x}) - \mathbf{F}_{\text{rep}}(\mathbf{x})$ when Proposition 4 applies to a single-integrator dynamical model.

Remark 5. Note that $\mathbf{u}_{\text{APF-AC}}$ given in (29) has strict safety guarantees. Firstly, as depicted in Fig. 1, the system remains safe when $\rho(\mathbf{x}) \geq \rho_0$. Then it remains to consider the case $\rho(\mathbf{x}) < \rho_0$. As shown in the proof of Proposition 4, we have $\tilde{c}(\mathbf{x}) = L_{\mathbf{f}}B(\mathbf{x}) + \|\mathbf{F}_{\text{rep}}(\mathbf{x})\|^2$, $\mathbf{d}(\mathbf{x}) = \mathbf{F}_{\text{rep}}(\mathbf{x})^\top$, and $\Gamma(\mathbf{x}) =$

$\|\mathbf{F}_{\text{rep}}(\mathbf{x})\|^2 + \alpha(h(\mathbf{x}))$. Then the control law $\mathbf{n}_{\text{AC}}(\mathbf{x})$ in (29) can be computed as:

$$\mathbf{n}_{\text{AC}}(\mathbf{x}) = -\frac{\tilde{c}(\mathbf{x}) + \mathbf{d}(\mathbf{x})\mathbf{u}_{\text{CLF}}}{\|\mathbf{d}(\mathbf{x})\|^2} \mathbf{d}(\mathbf{x})^\top. \quad (30)$$

By substituting $\mathbf{n}_{\text{AC}}(\mathbf{x})$ into the RCBF condition (12b), it gives

$$\begin{aligned} c(\mathbf{x}) + \mathbf{d}(\mathbf{x})\mathbf{u} &= -\Gamma(\mathbf{x}) - \mathbf{d}(\mathbf{x})\mathbf{u}_{\text{CLF}} \\ &= -\alpha(h(\mathbf{x})) - \|\mathbf{F}_{\text{rep}}(\mathbf{x})\|^2 - \mathbf{F}_{\text{rep}}(\mathbf{x})^\top \mathbf{u}_{\text{CLF}} \\ &< 0. \end{aligned}$$

This is due to that, when $h(\mathbf{x}) = 0$ (indicating that the robot arrives at the boundary of the obstacle), we have $\|\mathbf{F}_{\text{rep}}(\mathbf{x})\| = \infty$ as shown in (6). Consequently, the RCBF condition (12) is satisfied at all times with the control law $\mathbf{u}_{\text{APF-AC}}$ given in (29), which is aligned with the conclusion in Remark 2.

V. SIMULATION STUDIES

We use a reach-avoid navigation example [17] to show the efficacy of the special CBF-QP safety filter, i.e., (28), and the generalized APF-designed controller $\mathbf{u}_{\text{APF-AC}}$ presented in (29). In particular, we consider the following dynamical model with a control-affine structure for a robot, which is adapted from [22, Example 1].¹

$$\begin{aligned} \dot{x}_1 &= x_2 + u_1, \\ \dot{x}_2 &= x_1 + u_2, \end{aligned} \quad (31)$$

where $\mathbf{x} = [x_1, x_2]^\top$, $\mathbf{u} = [u_1, u_2]^\top$, $\mathbf{f}(\mathbf{x}) = [x_2, x_1]^\top$, and $\mathbf{g}(\mathbf{x}) = [1, 0; 0, 1]$. The robot begins at the initial position $\mathbf{x}_0 = (0, 0)$ and aims to reach the goal position $\mathbf{x}_{\text{goal}} = (3, 5)$. Additionally, three obstacles are present at $\mathbf{x}_{\text{O}_1} = (1, 1.5)$, $\mathbf{x}_{\text{O}_2} = (2.5, 3)$, and $\mathbf{x}_{\text{O}_3} = (4, 4.2)$. The basic settings for defining the attractive potential in (2) and repulsive potential in (4) are given as follows: $K_{\text{att}} = K_{\text{rep}} = 1$, $r = 0.5$, $\alpha(h(\mathbf{x})) = h(\mathbf{x})$. Following this, we utilize the attractive potential field defined in (2) and the repulsive potential field expressed in (4) to serve as the CLF and RCBF, respectively. Subsequently, using (10), (12), (13), and (24), we obtain:

$$\begin{aligned} a(\mathbf{x}) &= L_{\mathbf{f}}V(\mathbf{x}) = (\mathbf{x} - \mathbf{x}_{\text{goal}})^\top \cdot \mathbf{f}(\mathbf{x}), \\ \tilde{a}(\mathbf{x}) &= a(\mathbf{x}) + \|\mathbf{b}(\mathbf{x})\|^2, \\ \mathbf{b}(\mathbf{x}) &= L_{\mathbf{g}}V(\mathbf{x}) = (\mathbf{x} - \mathbf{x}_{\text{goal}})^\top \cdot \mathbf{g}(\mathbf{x}), \\ c(\mathbf{x}) &= L_{\mathbf{f}}B(\mathbf{x}) - \alpha(h(\mathbf{x})) = \mathbf{F}_{\text{rep}}(\mathbf{x})^\top \cdot \mathbf{f}(\mathbf{x}) - \alpha(h(\mathbf{x})), \\ \tilde{c}(\mathbf{x}) &= c(\mathbf{x}) + \Gamma(\mathbf{x}), \\ \Gamma(\mathbf{x}) &= \|\mathbf{F}_{\text{rep}}(\mathbf{x})\|^2 + \alpha(h(\mathbf{x})), \\ \mathbf{d}(\mathbf{x}) &= L_{\mathbf{g}}B(\mathbf{x}) = \mathbf{F}_{\text{rep}}(\mathbf{x})^\top \cdot \mathbf{g}(\mathbf{x}), \end{aligned}$$

where $\mathbf{F}_{\text{rep}}(\mathbf{x})^\top$ is given in (6). According to Lemma 4, we calculate the nominal control law for stabilization as given in (25), which yields \mathbf{u}_{CLF} . Next, the special CBF-QP safety filter \mathbf{u}_{AC} and the generalized APF-designed controller $\mathbf{u}_{\text{APF-AC}}$ are given in (28) and (29), respectively.

As shown in Figure 2, the nominal control \mathbf{u}_{nom} achieves the goal position without providing safety guarantees. To

¹The simulation code is available at: https://github.com/lyric12345678/A_Comparative_Study.git.

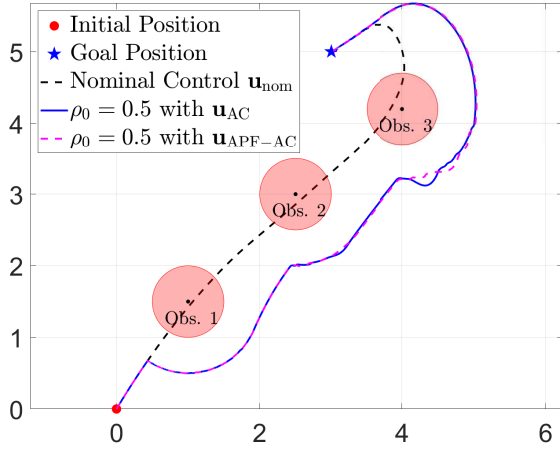


Fig. 2. A comparison of the reach-avoid performance for the nominal control \mathbf{u}_{nom} , the special CBF-QP safety filter \mathbf{u}_{AC} , and the generalized APF-designed controller $\mathbf{u}_{\text{APF-AC}}$ with $\rho_0 = 0.5$

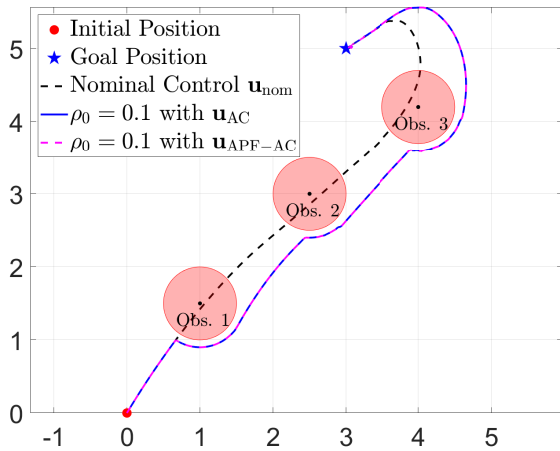


Fig. 3. A comparison of the reach-avoid performance for the nominal control \mathbf{u}_{nom} , the special CBF-QP safety filter \mathbf{u}_{AC} , and the generalized APF-designed controller $\mathbf{u}_{\text{APF-AC}}$ with $\rho_0 = 0.1$.

address this, we employ the special CBF-QP safety filter \mathbf{u}_{AC} and the generalized APF-designed controller $\mathbf{u}_{\text{APF-AC}}$ for the reach-avoid task. By setting $\rho_0 = 0.5$, both \mathbf{u}_{AC} and $\mathbf{u}_{\text{APF-AC}}$ can effectively tackle the reach-avoid challenge. However, minor differences can be observed in the trajectories regulated by the two controllers. This discrepancy arises due to Assumption 2 generally does not hold with $\rho_0 = 0.5$, rendering the two controllers are not equivalent. However, in Figure 3, we notice that both controllers not only ensure the successful implementation of the reach-avoid task but also have overlapping trajectories. This is because, when $\rho_0 = 0.1$, Assumption 2 is nearly satisfied at all times, thereby establishing equivalence between \mathbf{u}_{AC} and $\mathbf{u}_{\text{APF-AC}}$, as demonstrated in Proposition 4.

VI. CONCLUSIONS

This paper has established a bridge between two prevalent methodologies in motion planning: APFs and CBFs. By integrating APF information into the CBF-QP framework, we demonstrate that the APF-designed controllers can be derived from CBF-QP safety filters. This integration not only showcases the relationship between the two approaches but also provides a constructive method to derive special CBF-QP safety filters. We then extend the applicability of APF to a broader class of dynamical models featuring control-affine structures. Through a reach-avoid navigation example, we have illustrated the efficacy of the proposed methods.

APPENDIX A PROOF OF LEMMA 1

The Lagrangian of (14) is:

$$\mathcal{L}(\mathbf{x}, \mathbf{u}, \lambda) = \frac{1}{2} \|\mathbf{u} - \mathbf{u}_{\text{nom}}\|^2 + \lambda(\tilde{c}(\mathbf{x}) + \mathbf{d}(\mathbf{x})\mathbf{u}). \quad (32)$$

According to the Karush-Kuhn-Trucker (KKT) conditions [23], we know that

$$\frac{\partial \mathcal{L}}{\partial \mathbf{u}} = (\mathbf{u} - \mathbf{u}_{\text{nom}})^\top + \lambda \mathbf{d}(\mathbf{x}) = 0, \quad (33a)$$

$$\Rightarrow \mathbf{u} = \mathbf{u}_{\text{nom}} - \lambda \mathbf{d}(\mathbf{x})^\top,$$

$$\lambda F = \lambda(\tilde{c}(\mathbf{x}) + \mathbf{d}(\mathbf{x})\mathbf{u}) = 0, \quad (33b)$$

where $F = \tilde{c}(\mathbf{x}) + \mathbf{d}(\mathbf{x})\mathbf{u}$.

Consequently, we need to consider the following three cases.

Case 1. *The tightened CBF condition (14b) is not activated.*

In this case, we know that

$$\tilde{c}(\mathbf{x}) + \mathbf{d}(\mathbf{x})\mathbf{u} < 0, \quad (34a)$$

$$\lambda = 0, \quad (34b)$$

Substituting (34b) into (33a) and (34a) gives $\mathbf{u}_{\text{CBF}} = \mathbf{u}_{\text{nom}}$ and defines the domain set to be $\mathcal{S}_{\text{CBF-1}} = \{\mathbf{x} \in \mathbb{R}^n | \tilde{c}(\mathbf{x}) + \mathbf{d}(\mathbf{x})\mathbf{u}_{\text{nom}} < 0\}$.

Case 2. $\mathbf{b}(\mathbf{x}) \neq \mathbf{0}$. *The tightened CBF condition (14b) is activated.*

In this case, we know that

$$\tilde{c}(\mathbf{x}) + \mathbf{d}(\mathbf{x})\mathbf{u} = 0, \quad (35a)$$

$$\lambda \geq 0, \quad (35b)$$

By substituting (33a) into (35a), it gives

$$\lambda = \frac{\varphi(\mathbf{x})}{\|\mathbf{d}(\mathbf{x})\|^2}, \quad \mathbf{u}_{\text{CBF}} = \mathbf{n}(\mathbf{x}),$$

where $\varphi(\mathbf{x})$ and $\mathbf{n}(\mathbf{x})$ are defined in (16). Furthermore, with the condition (35b), we know the domain set is $\mathcal{S}_{\text{CBF-2}} = \{\mathbf{x} \in \mathbb{R}^n | \varphi(\mathbf{x}) \geq 0 \text{ and } \mathbf{d}(\mathbf{x}) \neq \mathbf{0}\}$.

Case 3. $\mathbf{d}(\mathbf{x}) = \mathbf{0}$.

In Case 2, $\mathbf{d}(\mathbf{x}) = \mathbf{0}$ gives $\mathbf{u} = \mathbf{u}_{\text{nom}}$ according to (33a). Then the condition (35a) defines the domain set to be $\tilde{\mathcal{S}}_{\text{CBF-1}} = \{\mathbf{x} \in \mathbb{R}^n | \varphi(\mathbf{x}) = 0 \text{ and } \mathbf{d}(\mathbf{x}) = \mathbf{0}\}$.

Combining Case 1, Case 2, and Case 3, we obtain the results in (14).

REFERENCES

- [1] L. C. Santos, F. N. Santos, E. S. Pires, A. Valente, P. Costa, and S. Magalhães, "Path planning for ground robots in agriculture: A short review," in *2020 IEEE International Conference on Autonomous Robot Systems and Competitions (ICARSC)*. IEEE, 2020, pp. 61–66.
- [2] Z. Liu, H. Wang, H. Wei, M. Liu, and Y.-H. Liu, "Prediction, planning, and coordination of thousand-warehousing-robot networks with motion and communication uncertainties," *IEEE Transactions on Automation Science and Engineering*, vol. 18, no. 4, pp. 1705–1717, 2020.
- [3] M. Ginesi, D. Meli, A. Roberti, N. Sansonetto, and P. Fiorini, "Autonomous task planning and situation awareness in robotic surgery," in *2020 IEEE/RSJ International Conference on Intelligent Robots and Systems (IROS)*. IEEE, 2020, pp. 3144–3150.
- [4] J.-K. Huang and J. W. Grizzle, "Efficient anytime CLF reactive planning system for a bipedal robot on undulating terrain," *IEEE Transactions on Robotics*, 2023.
- [5] O. Khatib, "Real-time obstacle avoidance for manipulators and mobile robots," *The International Journal of Robotics Research*, vol. 5, no. 1, pp. 90–98, 1986.
- [6] P. Vadakkepat, K. C. Tan, and W. Ming-Liang, "Evolutionary artificial potential fields and their application in real time robot path planning," in *Proceedings of the 2000 Congress on Evolutionary Computation*, vol. 1. IEEE, 2000, pp. 256–263.
- [7] F. Bounini, D. Gingras, H. Pollart, and D. Gruyer, "Modified artificial potential field method for online path planning applications," in *2017 IEEE Intelligent Vehicles Symposium (IV)*. IEEE, 2017, pp. 180–185.
- [8] S. M. H. Rostami, A. K. Sangaiah, J. Wang, and X. Liu, "Obstacle avoidance of mobile robots using modified artificial potential field algorithm," *EURASIP Journal on Wireless Communications and Networking*, vol. 2019, no. 1, pp. 1–19, 2019.
- [9] J. Ren, K. A. McIsaac, and R. V. Patel, "Modified Newton's method applied to potential field-based navigation for mobile robots," *IEEE Transactions on Robotics*, vol. 22, no. 2, pp. 384–391, 2006.
- [10] G. Li, A. Yamashita, H. Asama, and Y. Tamura, "An efficient improved artificial potential field based regression search method for robot path planning," in *2012 IEEE International Conference on Mechatronics and Automation*. IEEE, 2012, pp. 1227–1232.
- [11] Y.-b. Chen, G.-c. Luo, Y.-s. Mei, J.-q. Yu, and X.-l. Su, "UAV path planning using artificial potential field method updated by optimal control theory," *International Journal of Systems Science*, vol. 47, no. 6, pp. 1407–1420, 2016.
- [12] A. D. Ames, X. Xu, J. W. Grizzle, and P. Tabuada, "Control barrier function based quadratic programs for safety critical systems," *IEEE Transactions on Automatic Control*, vol. 62, no. 8, pp. 3861–3876, 2016.
- [13] X. Xu, P. Tabuada, J. W. Grizzle, and A. D. Ames, "Robustness of control barrier functions for safety critical control," *IFAC-PapersOnLine*, vol. 48, no. 27, pp. 54–61, 2015.
- [14] W. Xiao and C. Belta, "High-order control barrier functions," *IEEE Transactions on Automatic Control*, vol. 67, no. 7, pp. 3655–3662, 2021.
- [15] S.-C. Hsu, X. Xu, and A. D. Ames, "Control barrier function based quadratic programs with application to bipedal robotic walking," in *2015 American Control Conference (ACC)*. IEEE, 2015, pp. 4542–4548.
- [16] L. Lindemann and D. V. Dimarogonas, "Control barrier functions for signal temporal logic tasks," *IEEE Control Systems Letters*, vol. 3, no. 1, pp. 96–101, 2018.
- [17] A. Singletary, K. Klingebiel, J. Bourne, A. Browning, P. Tokumaru, and A. Ames, "Comparative analysis of control barrier functions and artificial potential fields for obstacle avoidance," in *2021 IEEE/RSJ International Conference on Intelligent Robots and Systems (IROS)*. IEEE, 2021, pp. 8129–8136.
- [18] P. Jagtap, G. J. Pappas, and M. Zamani, "Control barrier functions for unknown nonlinear systems using Gaussian processes," in *2020 59th IEEE Conference on Decision and Control (CDC)*. IEEE, 2020, pp. 3699–3704.
- [19] E. D. Sontag, "A 'universal' construction of Artstein's theorem on nonlinear stabilization," *Systems & Control Letters*, vol. 13, no. 2, pp. 117–123, 1989.
- [20] A. D. Ames, X. Xu, J. W. Grizzle, and P. Tabuada, "Control barrier function based quadratic programs for safety critical systems," *IEEE Transactions on Automatic Control*, vol. 62, no. 8, pp. 3861–3876, 2016.
- [21] M. H. Cohen, T. G. Molnar, and A. D. Ames, "Safety-critical control for autonomous systems: Control barrier functions via reduced-order models," *Annual Reviews in Control*, vol. 57, p. 100947, 2024.
- [22] X. Tan and D. V. Dimarogonas, "On the undesired equilibria induced by control barrier function based quadratic programs," *Automatica*, vol. 159, p. 111359, 2024.
- [23] E. K. Chong, W.-S. Lu, and S. H. Zak, *An Introduction to Optimization: With Applications to Machine Learning*. John Wiley & Sons, 2023.